Letters

Current Ripple Amplitude Measurement in Multiphase Power Converters

Paula Cervellini, Pablo Antoszczuk, Rogelio García Retegui, and Marcos Funes

***Abstract*—Improvements in the total current ripple in interleaved power converters are mainly determined by differences between the phase inductor values. Several methods have been presented in the literature to mitigate this problem, which requires the knowledge of the relative current ripple amplitude. However, in these methods, the measurement of such an amplitude is not addressed. This characteristic is difficult to measure because of the switching noise and the necessity to precisely locate the current waveforms peaks, despite the switches and drivers delay. Furthermore, the above-mentioned methods either perform the correction in real time or in a self-commissioning state. Therefore, it is necessary to implement the amplitude measurement in the same platform as the current control, which implies that the computational overhead should be minimized. This work presents a methodology for the measurement of the ratio among phase current ripple amplitudes in the frequency domain. The proposal allows us to precisely determine this characteristic, with a reduced sampling frequency and high noise immunity. Experimental tests on a four-phase buck converter validate the proposal.**

***Index Terms*—Current ripple, power converters, signal processing.**

I. Introduction

MULTIPHASE power converters consist of the parallel connection of M equal converters in such a way that the total current i_T is divided among M paths or phases. When compared to a single converter, multiphase converters reduce switching and conduction losses by dividing the total current among phases. They also improve total current ripple (Δi_T) characteristics, including amplitude reduction and frequency increase to M times the switching frequency $f_{\rm sw}$, by interleaving each phase current ripple [1], [2]. Therefore, filtering requirements are reduced in the common point among phases, as the minimum frequency is $M f_{\rm sw}$.

However, the above-mentioned features can be affected by various practical implementation factors, such as tolerances and parasitic elements on the converter passive and active components. In this sense, series voltage drop on switching devices and inductor parasitic resistance could produce mismatch on the mean current among phases [3]. Nevertheless, this effect, as well as the nonideal phase shift produced by delays on switching devices and drivers, can be mitigated by means of control techniques [2], [4], [5]. Furthermore, as inductance value tolerance may reach $\pm 5\,\%$ to $\pm 10\,\%$ [6], differences on each phase current ripple amplitude are generated, which impacts on the total current ripple characteristics [7], [8]. Under this condition, the switching frequency component $f_{\rm sw}$ and its $M-1$ harmonics are not canceled in Δi_T. As a consequence, if the filter is designed to attenuate the $M f_{\rm sw}$ component, the voltage ripple amplitude is increased in the common point among phases. This problem becomes more significant as the number of phases increases, as the difference between the expected minimum frequency and the switching frequency increases.

Several strategies have been presented in the literature to mitigate the effect of differences among the phase inductors. In [8], it is proposed to modify the switching sequence, in such a way that similar amplitude phase current ripples are shifted 180°, which reduces $f_{\rm sw}$ component in the total ripple. This principle is extended to any phase number and its results are improved in [9] by using an objective function for the optimization procedure. On the other hand, in [10] and [11], it is proposed to modify the ideal phase shift ($2\pi/M$) to cancel $f_{\rm sw}$ component and its harmonics in the total ripple. All these strategies rely on the precise knowledge of the ratio among the phase current ripple amplitudes; however, the measurement methodology is not discussed.

In this sense, the measurement of the current ripple amplitude presents several issues illustrated in Fig. 1. This figure shows the phase current ripple ($i_{\rm phase}$) affected by the high-frequency noise produced by the switching device and the converter parasitic elements. It also presents the sampled version ($i^*_{\rm phase}$) using a sampling frequency $f_s = 20 f_{\rm sw}$.

As can be noted in Fig. 1, in order to determine the amplitude, the measurement must be performed in the switching instants. However, the location of these instants varies depending on the input and output voltages. One possible option to determine the amplitude is to synchronize the sampling instant with the switching signal. Nevertheless, as previously stated, this approach can be affected by the switching noise, which requires the knowledge of the measurement circuit bandwidth and the different system delays, in order to reach the synchronization.

Manuscript received December 21, 2016; revised February 14, 2017; accepted March 20, 2017. Date of publication March 23, 2017; date of current version April 24, 2017. This work was supported in part by the Universidad Nacional de Mar del Plata, Argentina, the Consejo Nacional de Investigaciones Cientificas y Tecnologicas project PIP 0210, Argentina, by the Ministerio de Ciencia, Tecnologia e Innovacion Productiva, Argentina, and by the Agencia Nacional de Promoción Cientifica y Tecnologica, Argentina.

The authors are with the Facultad de Ingenieria, Instituto de Investigaciones Cientificas y Tecnologicas en Electronica, Consejo Nacional de Investigaciones Cientificas y Tecnologicas, Universidad Nacional de Mar del Plata, 7600 Mar del Plata, Argentina (e-mail: paulacervellini@fi.mdp.edu.ar; pablo_ant@fi.mdp.edu.ar; rgarcia@fi.mdp.edu.ar; mfunes@fi.mdp.edu.ar).

Digital Object Identifier 10.1109/TPEL.2017.2686784

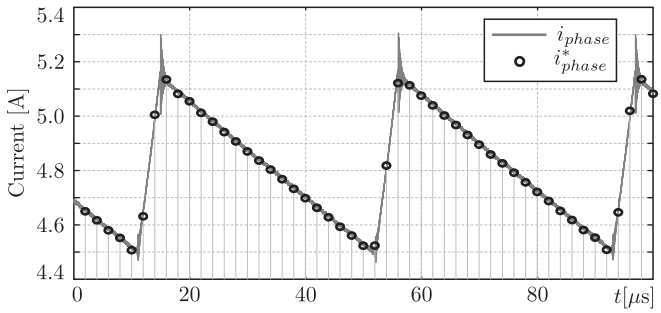

Fig. 1. Phase current ripple ($i_{\rm phase}$) and sampled current ripple with $f_s = 20 f_{\rm sw}$ ($i^*_{\rm phase}$).

The above-mentioned problem in the amplitude measurement can be reduced by using frequency-domain methods [12], which allow us to increase the noise rejection and are independent of the switching instant. Since correction strategies are intended as online or self-commissioning methodologies, the amplitude measurement should be implemented in the same platform as the current control. This requirement implies that the measurement should be performed without increasing the computational overhead of the digital platform.

Considering the aforementioned issues, this work presents a methodology for measuring the ratio among the phase current ripple values in interleaved converters in the frequency domain. The proposed method allows us to determine said amplitude with high immunity to the switching noise and a reduced number of points, consequently reducing the memory use and sampling frequency. Furthermore, the proposed method can be used both in the continuous conduction mode (CCM) and the discontinuous conduction mode (DCM). The proposal is experimentally validated using a four-phase buck converter.

II. Proposed Method

The proposed method is based on the frequency-domain analysis of each phase current ripple. In order to perform such analysis, the following is assumed:

1) the converter operates in the steady state;
2) the current ripple is approximated as linear segments, as the time constant associated with the inductor and its resistive component is much higher than the switching period T [13], [14];
3) all phases have the same waveform, same period T, and switch turn-on time $T_{\rm on}$;
4) the sampling signal period can be precisely defined, provided the timing accuracy of modern digital platforms [15];
5) windowing problems in the frequency-domain analysis are neglected, as control signals and sampling instants are generated on the same digital platform.

Under these considerations, each phase ripple can be considered as a piecewise linear function with different slopes. Therefore, current ripple can be defined as a triangular function when the converter is operating in the CCM, or as a triangular function with dead time when operating in the DCM. Fig. 2

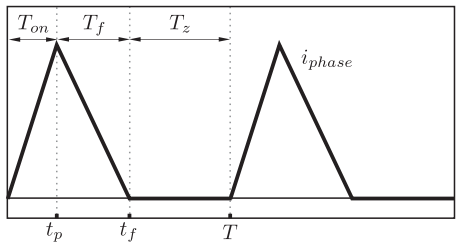

Fig. 2. Inductor current ripple for the DCM case.

shows the waveform for the DCM case. In this case, the switch is ON during $T_{\rm on}$ interval and turns OFF in $t = t_p$. During T_f interval, the switch is OFF, but the current is greater than zero until instant t_f, where it starts the dead time of length T_z. The CCM case can be considered as a particular DCM case with no dead time, i.e., $t_f = T$. The duty cycle is defined for the CCM case as $d = t_p/T$.

Once the current ripple waveform is defined, its harmonic content can be evaluated. Since the module of each frequency component of a given periodic signal is proportional to its peak-to-peak amplitude, $\Delta i_{\rm phase}$ in this case, then

$$c_{1_{\rm DCM}} = \Delta i_{\rm phase}/K_{\rm DCM} \tag{1}$$

$$c_{1_{\rm CCM}} = \Delta i_{\rm phase}/K_{\rm CCM} \tag{2}$$

where $c_{1_{\rm DCM}}$ and $c_{1_{\rm CCM}}$ are the modules of the switching frequency components for DCM and CCM cases, respectively, whereas $K_{\rm DCM}$ and $K_{\rm CCM}$ are proportionality factors that depend on the current ripple shape, i.e., DCM or CCM operation.

Furthermore, the switching frequency component for a given conduction mode can be calculated by using the Fourier series as

$$c_1 = \frac{1}{T}\left|\int_0^T i_{\rm phase}(t).e^{-j2\pi t/T}\ dt\right|. \tag{3}$$

As previously stated, $T_{\rm on}$, T_f, and T_z are the same on all phases for a given DCM converter, and d is the same along phases for a given CCM converter [16]. Therefore, the ratio between the peak-to-peak amplitude of two given phases is equal to the ratio between the amplitude of their respective switching frequency components. In order to verify that this factor is constant among the different phases, $K_{\rm DCM}$ and $K_{\rm CCM}$ are calculated using (3) for the DCM and the CCM

$$\begin{aligned} K_{\rm DCM} = \pi[&a^2 + b^2 + c^2 - 2ab\cos(\omega_{\rm sw}(t_f - t_p)) \\ &+ 2bc\cos(\omega_{\rm sw}.t_f) - 2ac\cos(\omega_{\rm sw}.t_p)]^{(-1/2)} \end{aligned} \tag{4}$$

where

$$\omega_{\rm sw} = \frac{2\pi}{T}, \qquad a = \frac{1}{\omega_{\rm sw}}\frac{t_f}{t_p(t_f - t_p)}$$

$$b = \frac{1}{\omega_{\rm sw}}\frac{1}{t_f - t_p}, \qquad c = \frac{1}{\omega_{\rm sw}}\frac{1}{t_p}.$$

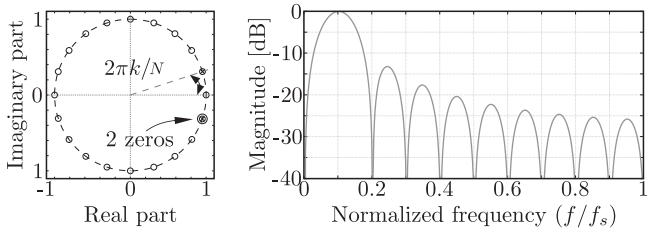

Fig. 3. SGT z-plane singularities and frequency response. $k = 1$ and $N = 20$.

Given that, in the CCM, $t_f = T$ and $d = t_p/T$, $K_{\rm CCM}$ is simplified as

$$K_{\rm CCM} = \frac{\pi^2 d(1-d)}{\sin(\pi d)}. \tag{5}$$

As can be noted, (4) and (5) depend on the switching period T and instants t_p and t_f, which are equal in all phases. Therefore, the ratio between the peak-to-peak amplitude of two given phases can be calculated as the ratio between their switching frequency components. For example, for phases 1 and 2 corresponding to a DCM operating converter, the amplitude ratio is calculated as

$$\frac{\Delta i_{\rm phase_1}}{\Delta i_{\rm phase_2}} = \frac{c_{1_{1_{\rm DCM}}}}{c_{1_{2_{\rm DCM}}}}. \tag{6}$$

From the previous analysis, it can be concluded that the phase amplitude ratio is equal to the switching component ratio. Consequently, a suitable frequency-domain method for this purpose is the sliding Goertzel transform (SGT), which allows the efficient calculation of a single-frequency component in real time [12], [17]. The transfer function of the SGT of length N, configured to calculate the kth order frequency component, is shown as follows [18]:

$$H_{\rm SGT}(z) = \frac{(1-z^{-N})(1-e^{-j2\pi k/N}z^{-1})}{1-2\cos(2\pi k/N)z^{-1}+z^{-2}}. \tag{7}$$

As can be noted, $H_{\rm SGT}$ singularities in the z-plane are composed of N zeros on the unity circle, produced by the sliding window of length N, an additional zero on $e^{-j2\pi k/N}$, and two poles on $e^{\pm j2\pi k/N}$. Fig. 3 shows the distribution of poles and zeros in the z-plane, and the frequency response for a $k = 1$ and $N = 20$ filter. As can be seen, as sampling frequency can be precisely set as a function of switching frequency, $H_{\rm SGT}$ provides N transmission zeros located at the $f_{\rm sw}$ harmonics, other than the central frequency, defined by k.

However, the representation of this function coefficients in systems with finite precision arithmetic may yield an incorrect cancellation among zeros and poles. Furthermore, rounding errors may produce that the singularities are moved outside the unity circle, thus affecting the system stability. In order to ensure stability, it is necessary to introduce a damping coefficient to move the singularities back inside the unity circle [18]. Even though this methodology ensures stability, the attenuation at frequencies others than the central frequency is reduced and the phase response is distorted [19].

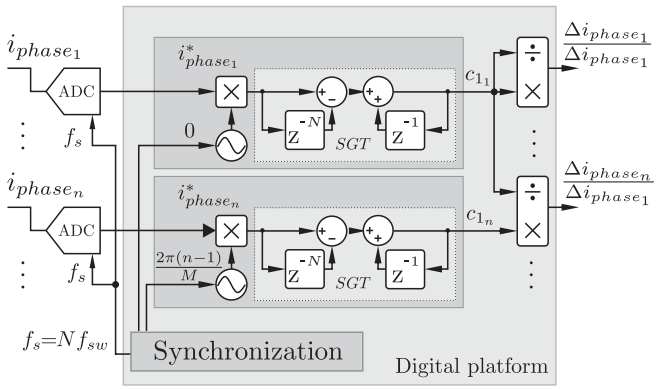

Fig. 4. Proposed method block diagram.

In [20], previously mentioned stability issues are avoided configuring the SGT to calculate the dc level ($k = 0$), since it is not necessary to represent any coefficient different than 1, as

$$H_{\rm SGT}(z) = \frac{(1-z^{-N})}{(1-z^{-1})}. \tag{8}$$

In this sense, if the signal under test is multiplied by another signal with the same frequency as the harmonic of interest [20], a dc value proportional to the current ripple amplitude can be obtained. As an example, in (9), the result of the multiplication of two signals V_1 and V_2 is shown, proving that the result, $V_0(t)$, has a continuous current (dc) component only when w_1 and w_2 are equal

$$\begin{aligned} V_0(t) &= V_1(t).V_2(t) \\ &= \frac{A_1.A_2}{2}\left[\cos\left((w_1+w_2)t+\phi\right)\right. \\ &\quad \left.+\cos\left((w_1-w_2)t+\phi\right)\right]. \end{aligned} \tag{9}$$

Fig. 4 summarizes the proposed method to obtain the ratio between phase 1 and a generic phase n current ripples. In this diagram, it is shown that $i_{\rm phase}$ is sampled at $f_s = Nf_{\rm sw}$ to obtain $i^*_{\rm phase}$. Then, $i^*_{\rm phase}$ is multiplied by a signal with the same frequency as the switching frequency, and phase-shift equal to the corresponding phase, i.e., 0 for phase 1, $2\pi/M$ for phase 2, and so on. Moreover, by means of the SGT filter with $k = 0$, the dc component is obtained. Finally, the ratio among phases is obtained by dividing the $f_{\rm sw}$ component of each phase by the $f_{\rm sw}$ component of the phase selected as a reference (phase 1 in this case).

III. Experimental Results

The proposed method validation has been performed using signals acquired from a four-phase buck converter, operating in the CCM and the DCM. The switching period is $T = 40.96\,\mu$s. The duty cycle for the CCM case is $d = 0.09$, whereas, for the DCM case, $t_p = 13.5\,\mu$s and $t_f = 28.1\,\mu$s. The duty cycle for the CCM has been selected to test the measurement methodology in a critical case, where one of the current ripple slopes is much larger than the other.

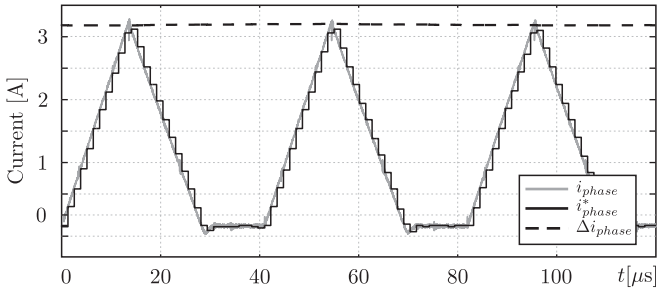

Fig. 5. DCM operation. Current and sampled current with the obtained amplitude.

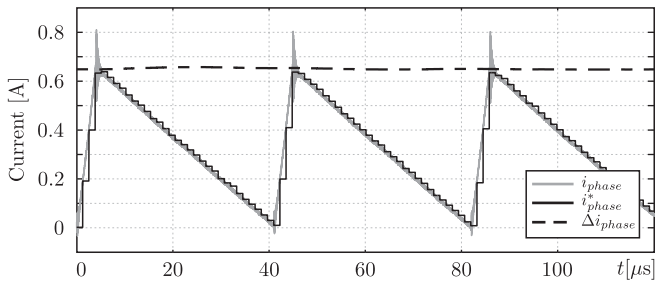

Fig. 6. CCM operation. Current and sampled current with the obtained amplitude.

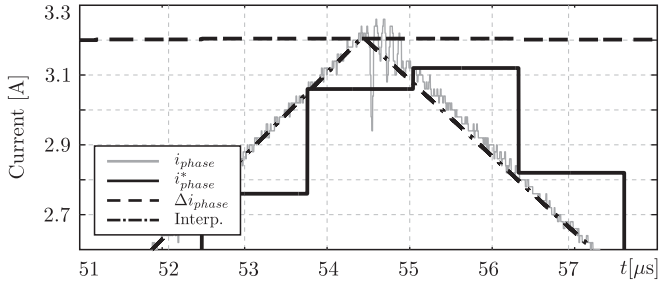

Fig. 7. DCM Operation. Proposed method and linear regression.

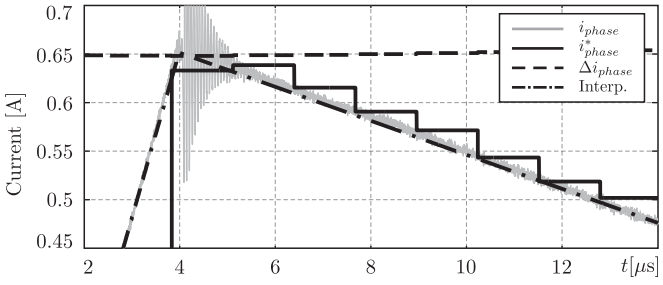

Fig. 8. CCM Operation. Proposed method and linear regression.

First, in order to illustrate the testing methodology and verify expressions (1) and (2), the ripple amplitude for a single phase is calculated. For this purpose, constants K_{DCM} (4) and K_{CCM} (5) must be calculated using the parameters described above

$$K_{\text{DCM}} = 2.18 \tag{10}$$

$$K_{\text{CCM}} = 2.9. \tag{11}$$

Once K_{DCM} and K_{CCM} are determined, the peak-to-peak amplitude for each case is calculated using a sampling period $T_s = T/32$. It should be pointed out that, since the switching signals are generated in a digital platform, it is simple to generate a sampling frequency multiple of the switching frequency. Therefore, windowing problems can be neglected. Figs. 5 and 6 show the current ripple, the sampled version, and the amplitude obtained using the proposed method for the DMC and CCM cases, respectively.

As can be noticed, the proposed method allows us to obtain the peak-to-peak amplitude in both cases. However, due to the switching noise, it is difficult to evaluate the method precision. In order to obtain an amplitude to be contrasted with the proposed method, a linear interpolation is calculated for the rising and falling segments, using a much higher sampling frequency $T_{s_{\text{int}}} = T/4096$. The peak value is then computed from the intersection between the two interpolations, as shown with dashed and dotted lines in Figs. 7 and 8. Finally, the value obtained using the proposed method, shown with dashed line in Figs. 7 and 8, is compared with the interpolation to compute the error. As the interpolation requires a much larger number of points, and given its computational complexity, it is not practical to implement the measuring system in the same platform as the current control. Therefore, it is only used for evaluating the proposed method. If this procedure is repeated for successive peaks in the current ripple, it can be determined that the error is between 0.15% and 1.1% for the DCM and $\pm 0.17\%$ for the CCM.

As can be observed, the error is larger for the DCM case, which is due to the inverse recovery phenomenon. This phenomenon has switching frequency components that add to the ones proportional to the current ripple amplitude. Precision in the DCM can be improved by disregarding negative current values. By using this procedure, the error is improved to $\pm 0.5\%$.

The multiphase case is evaluated using the previously presented methodology, i.e., comparing the results obtained using the proposed method with the interpolation for each phase. Fig. 9 shows the amplitudes ratio for the $M = 4$ converter in the DCM mode, obtained using the proposed method. In this case, as previously stated, the ratio among phase ripple amplitudes will be equal to the ratio among the switching frequency components. Thus, it is not necessary to calculate K_{DCM} or K_{CCM}.

It should be pointed out that the correction methods previously described have a much smaller bandwidth than the switching frequency. Therefore, in these methods, it is possible to use the average amplitude value. Then, if the previously described methodology is averaged ten consecutive switching cycles, the amplitude ratios yield

$$\begin{aligned}
\Delta i_{\text{phase}_1}/\Delta i_{\text{phase}_1} &= 1 \\
\Delta i_{\text{phase}_2}/\Delta i_{\text{phase}_1} &= 1.0016 \\
\Delta i_{\text{phase}_3}/\Delta i_{\text{phase}_1} &= 0.9955 \\
\Delta i_{\text{phase}_4}/\Delta i_{\text{phase}_1} &= 1.0254.
\end{aligned} \tag{12}$$

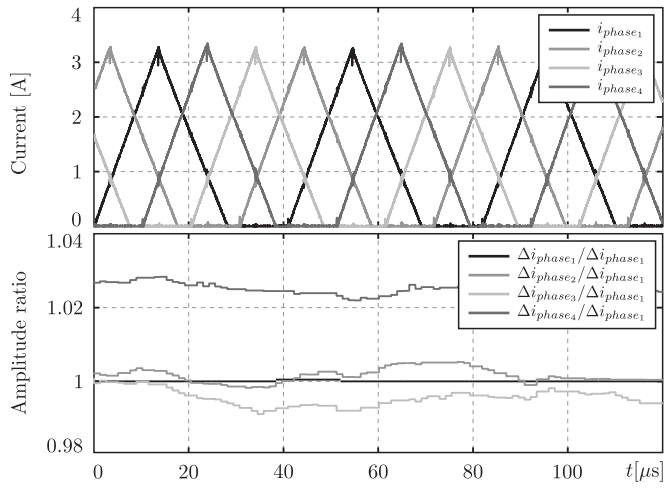

Fig. 9. DCM operation. (Top) Measured phase currents. (Bottom) Ripple amplitude ratios using the proposed method.

These amplitudes ratio can be compared with the amplitudes ratio obtained using the linear interpolation. If $\Delta i_{\mathrm{int}_j}$ is defined as the jth phase amplitude obtained using interpolation, the interpolated amplitude ratios result

$$\begin{aligned}\Delta i_{\mathrm{int}_1}/\Delta i_{\mathrm{int}_1} &= 1\\ \Delta i_{\mathrm{int}_2}/\Delta i_{\mathrm{int}_1} &= 1.0087\\ \Delta i_{\mathrm{int}_3}/\Delta i_{\mathrm{int}_1} &= 0.9998\\ \Delta i_{\mathrm{int}_4}/\Delta i_{\mathrm{int}_1} &= 1.0278. \end{aligned} \tag{13}$$

From previous results, it can be seen that the proposed method allows us to obtain the relative amplitudes with a precision smaller than 1%. Therefore, this method allows us to determine whether a given phase ripple amplitude is smaller or larger than the remaining ones. This information can then be used by compensation methodologies to reduce the impact on the total ripple.

IV. Conclusion

Difference among the phase inductor value is one of the main factors that affect the multiphase power converter performance, as it avoids the correct current ripple reduction and frequency increase. Available methodologies to mitigate this problem rely on the precise knowledge of the ratio among the phase ripple amplitudes. In this work, a methodology to measure this ratio has been presented. The proposed method is able to determine the relative current ripple amplitude with high immunity to the switching noise and a reduced number of points, based on the frequency-domain analysis of each phase current ripple. By means of tests on a four-phase buck converter, it has been determined that this methodology is capable of determining the ratio among phases with a precision better than 1%, when compared to the results obtained by using linear interpolation with a much larger number of points. Furthermore, as the required samples per period and computational overhead are reduced, the proposed method is suitable to be implemented in the same platform as the current control.

References

[1] R. G. Retegui, M. Benedetti, M. Funes, P. Antoszczuk, and D. Carrica, "Current control for high-dynamic high-power multiphase buck converters," *IEEE Trans. Power Electron.*, vol. 27, no. 2, pp. 614–618, Feb. 2012.

[2] O. García, P. Zumel, A. de Castro, and J. A. Cobos, "Automotive dc-dc bidirectional converter made with many interleaved buck stages," *IEEE Trans. Power Electron.*, vol. 21, no. 3, pp. 578–586, May 2006.

[3] O. García, P. Zumel, A. de Castro, P. Alou, and J. A. Cobos, "Current self-balance mechanism in multiphase buck converter," *IEEE Trans. Power Electron.*, vol. 24, no. 6, pp. 1600–1606, Jun. 2009.

[4] R. F. Foley, R. C. Kavanagh, and M. G. Egan, "Sensorless current estimation and sharing in multiphase buck converters," *IEEE Trans. Power Electron.*, vol. 27, no. 6, pp. 2936–2946, Jun. 2012.

[5] Y. Cho, A. Koran, H. Miwa, B. York, and J. S. Lai, "An active current reconstruction and balancing strategy with DC-link current sensing for a multi-phase coupled-inductor converter," *IEEE Trans. Power Electron.*, vol. 27, no. 4, pp. 1697–1705, Apr. 2012.

[6] A. Borrell, M. Castilla, J. Miret, J. Matas, and L. G. De Vicuña, "Control design for multiphase synchronous buck converters based on exact constant resistive output impedance," *IEEE Trans. Ind. Electron.*, vol. 60, no. 11, pp. 4920–4929, Nov. 2013.

[7] P. D. Antoszczuk, R. G. Retegui, N. Wassinger, S. Maestri, M. Funes, and M. Benedetti, "Characterization of steady-state current ripple in interleaved power converters under inductance mismatches," *IEEE Trans. Power Electron.*, vol. 29, no. 4, pp. 1840–1849, Apr. 2014.

[8] O. García, A. de Castro, P. Zumelis, and J. A. Cobos, "Digital-control-based solution to the effect of nonidealities of the inductors in multiphase converters," *IEEE Trans. Power Electron.*, vol. 22, no. 6, pp. 2155–2163, Nov. 2007.

[9] P. Antoszczuk, P. Cervellini, R. G. G. Retegui, and M. Funes, "Optimized switching sequence for multiphase power converters under inductance mismatch," *IEEE Trans. Power Electron.*, vol. 32, no. 3, pp. 1697–1702, Mar. 2017.

[10] M. Schuck and R. C. N. Pilawa-Podgurski, "Ripple minimization through harmonic elimination in asymmetric interleaved multiphase DC-DC converters," *IEEE Trans. Power Electron.*, vol. 30, no. 12, pp. 7202–7214, Dec. 2015.

[11] M. L. A. Caris, H. Huisman, J. M. Schellekens, and J. L. Duarte, "Generalized harmonic elimination method for interleaved power amplifiers," in *Proc. 38th Annu. Conf. IEEE Ind. Electron. Soc. Conf.*, 2012, pp. 4979–4984.

[12] J. F. Chicharo and M. T. Kilani, "A sliding Goertzel algorithm," *Signal Process.*, vol. 52, no. 3, pp. 283–297, Aug. 1996.

[13] M. Khazraei and M. Ferdowsi, "Modeling and analysis of projected cross point control—A new current-mode-control approach," *IEEE Trans. Ind. Electron.*, vol. 60, no. 8, pp. 3272–3282, Aug. 2013.

[14] P. D. Antoszczuk, R. G. Retegui, M. Funes, N. Wassinger, and S. Maestri, "Interleaved current control for multiphase converters with high dynamics mean current tracking," *IEEE Trans. Power Electron.*, vol. 31, no. 12, pp. 8422–8434, Dec. 2016.

[15] E. Monmasson, L. Idkhajine, M. N. Cirstea, I. Bahri, A. Tisan, and M. W. Naouar, "FPGAs in industrial control applications," *IEEE Trans. Ind. Informat.*, vol. 7, no. 2, pp. 224–243, May 2011.

[16] P. Cervellini, P. Antoszczuk, R. G. Retegui, M. Funes, and D. Carrica, "Steady state characterization of current ripple in DCM interleaved power converters," in *Proc. Argentine Conf. Micro-Nanoelectron., Technol. Appl.*, 2016, pp. 33–38.

[17] C. M. Orallo *et al.*"Harmonics measurement with a modulated sliding discrete Fourier transform algorithm," *IEEE Trans. Instrum. Meas.*, vol. 63, no. 4, pp. 781–793, Apr. 2014.

[18] E. Jacobsen and R. Lyons, "The sliding DFT," *IEEE Signal Process. Mag.*, vol. 20, no. 2, pp. 74–80, Mar. 2003.

[19] R. Garcia-Retegui, S. A. Gonzalez, M. A. Funes, and S. Maestri, "Implementation of a novel synchronization method using sliding Goertzel DFT," in *Proc. IEEE Int. Symp. Intell. Signal Process.*, Oct. 2007, pp. 1–5.

[20] K. Duda, "Accurate, guaranteed stable, sliding discrete Fourier transform [DSP tips & tricks]," *IEEE Signal Process. Mag.*, vol. 27, no. 6, pp. 124–127, Nov. 2010.